 doi:10.20944/preprints201807.0184.v1

Article

Heat and Mass Transfer Properties of Sugar Maple Wood Treated by the Thermo-Hygro-Mechanical Densification Process

Qilan Fu [1], Alain Cloutier [2,*] and Aziz Laghdir [3]

[1] Ph.D. Candidate, Center de recherche sur les matériaux renouvelables (Renewable Materials Research Center), Département des sciences du bois et de la forêt (Department of Wood and Forest Science), Université Laval, Québec, QC, Canada, G1V 0A6; qilan.fu.1@ulaval.ca

[2] Professor, Center de recherche sur les matériaux renouvelables (Renewable Materials Research Center), Département des sciences du bois et de la forêt (Department of Wood and Forest Science), Université Laval, Québec, QC, Canada, G1V 0A6; alain.cloutier@sbf.ulaval.ca

[3] Research scientist, Service de recherche et d'expertise en transformation des produits forestiers (Research and Expertise Service on Transformation of Forest Products), 25 Armand-Sinclair, Porte 5, Amqui, QC, Canada, G5J 1K3; aziz.laghdir@serex.qc.ca

* Correspondence: alain.cloutier@sbf.ulaval.ca; Tel.: +1-418-656-5851

Abstract: This study investigated the evolution of density, gas permeability and thermal conductivity of sugar maple wood during the thermo-hygro-mechanical densification process. The results suggested that the oven-dry average density of densified samples was significantly higher than that of the control samples. However, the oven-dry density did not show a linear increase with the decrease of wood samples thickness. The radial intrinsic gas permeability of the control samples was 5 to 40 times higher than that of densified samples, which indicated that the void volume of wood was reduced notably after the densification process. The thermal conductivity increased by 0.5 - 1.5% per percent increase of moisture content for densified samples. The thermal conductivity of densified wood was lower than that of the control samples. The densification time had significant effects on the oven-dry density and gas permeability. Both the densification time and the moisture content had significant effects on thermal conductivity, but their interaction effect was not significant.

Keywords: density; gas permeability; thermal conductivity; densification

1. Introduction

Heat and mass properties of wood or wood-based materials are essential characteristics required for a variety of purposes, including the modeling of densification process and the characterization of the densified wood as building materials. Among others, typical properties required are density, permeability and thermal conductivity. For modeling purposes, proper identification and input in terms of these properties are crucial for increasing the accuracy of predictions. However, during the thermo-hygro-mechanical (THM) densification process, density, permeability and thermal conductivity of wood are all time-dependent, which makes the identification of these parameters difficult.

Bulk flow is the principal mechanism for the transport of fluids through wood, which occurs through the voids of the wood under a static or capillary pressure gradient [1]. The bulk flow rate is determined by wood permeability. During the hot-pressing process of wood composite materials, the permeability controls the convective heat transfer from surface layers to the core layer and impacts the movement of the vapor from the core to the edges [2]. Since gas permeability depends largely on the pore structure of the fiber or particle mat, the densification treatment should have a direct effect on the permeability. Comstock [3] reported that the arrangement of wood principal directions have more important effects on its gas permeability than any other parameter. In some

 doi:10.20944/preprints201807.0184.v1

species, the longitudinal permeability could be 10^6 higher than in the transverse direction, due to the arrangement of the wood cells.

A few researchers investigated the gas permeability of wood based panels by experimental methods [4-8]. Almost all the methods described in the literature are based on measuring the amount of gas flow at a given pressure gradient applied across the sample. Defo et al. [9] measured radial and tangential gas permeability values of sugar maple wood (oven-dry density varied from 587 to 676 kg/m^3) between 2.04×10^{-17} m^3_{air} m^{-1} $_{moist\ wood}$ and 2.84×10^{-17} m^3_{air} m^{-1} $_{moist\ wood}$. Von Haas [6] reported that the MC had almost no effect for low density samples and a slight influence on samples with a density above 900 kg/m^3. Moreover, air permeability was at least two orders of magnitude higher than steam permeability, which might be due to the swelling of wood and the viscosity of the fluid on the superficial permeability [4,10].

Thermal conductivity is an important material property in determining the heat transfer rate [11]. The thermal conductivity of wood is affected by several basic factors: density, temperature, moisture content (MC), extractive content, grain direction, structural irregularities such as checks and knots and microfibril angle, of which the density and MC are predominant. The thermal conductivity of wood and wood-based composites is known to increase with MC, temperature, density, and extractive content [12]. Troppová et al. [13] found that higher temperature resulted in larger differences between the thermal conductivity values of wood-based fiberboards in the oven dry condition and at 14.2% MC. Thermal conductivity in the radial direction was reported to be about 5% to 10% higher than that in the tangential direction [14]. Thermal conductivity along the grain has been reported to be 1.5 to 2.8 times higher than that across the grain, but the reported values vary widely. For example, Maclean [15] found that the thermal conductivity along the longitudinal direction is about 2.25 to 2.75 times higher than transverse thermal conductivity with an average of approximately 2.5.

The steady-state method is normally applied to measure the thermal conductivity of wood [16]. A large number of empirical equations could be found in the literature, to describe the relationship between wood thermal conductivity, density and MC [1,6,10,15,17]. However, these empirical equations are applicable only within a limited range of MC and density levels. Hence, these relations may not be appropriate to describe the variation of the thermal conductivity of wood undergoing THM densification because both MC and density vary continuously during the process. In addition, little empirical data were found for the thermal conductivity of sugar maple wood at different density levels. Therefore, the objective of the current study was to investigate the variation of density, gas permeability and thermal conductivity of sugar maple wood during the THM densification process.

2. Materials and Methods

Thin sawn strips of sugar maple (*Acer saccharum* March.) wood provided by a hardwood flooring plant (Lauzon, Distinctive Hardwood Flooring Inc., Papineauville, Québec, Canada). Their average apparent density (20 °C and 65% relative humidity (RH)) was 734 kg/m^3 and their dimensions were 5.7 mm (radial) × 84.0 mm (tangential) × 695.0 mm (longitudinal). When they were received, the strips were stored in a conditioning room at 20 °C and 65% RH until an equilibrium moisture content of approximately 12% was achieved. Ten groups of 8 strips were densified for 0 (control sample), 5, 10, 15, 20, 25, 30, 35, 40 and 45 min, respectively. And were used for experimental determination of the evolution with time of the density, gas permeability and thermal conductivity during the THM densification process.

2.1. Thermo-hygro-mechanical densification process

A steam injection press (Dieffenbacher, Alpharetta, USA) with dimensions of 862 mm × 862 mm was used for the densification treatment (Figure 1a) [18]. Steam injection holes with a diameter of 1.5 mm were distributed uniformly at 32 mm intervals on both the upper and lower platens of the press (Figure 1b). To reduce wood surface carbonization and distribute the steam uniformly, both surfaces of the specimens were covered by a thin heat-resistant fabric permeable to steam made of Nomex®

 doi:10.20944/preprints201807.0184.v1

III A, manufactured by Dupont™ [19]. The two platens were preheated to the target temperature (200 °C) before treatment. The upper platen reached the specimens within 86 s (closing time).

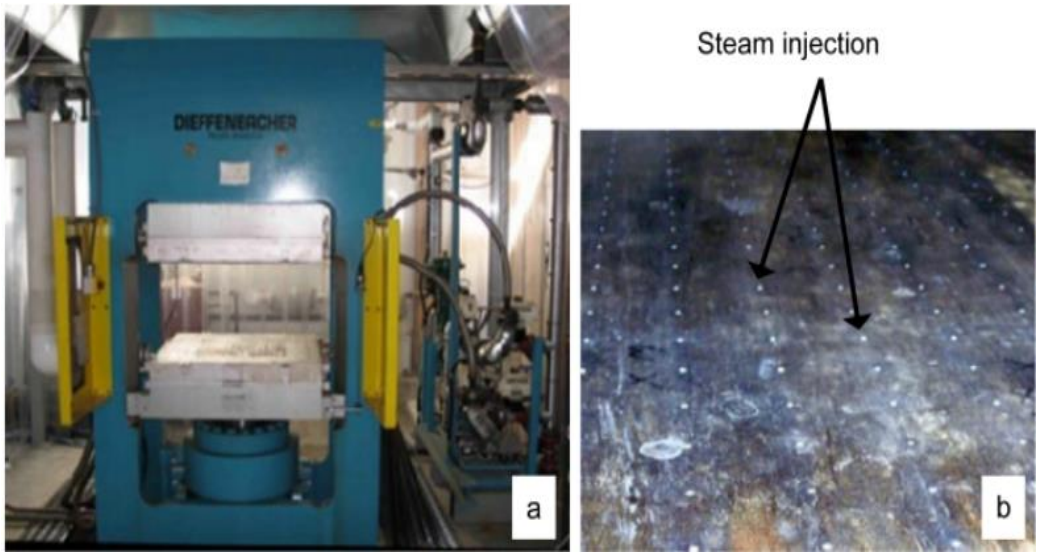

Figure 1. Steam injection hot press used for THM densification treatment. a) 862 mm × 862 mm hot press, b) press platen with steam injection holes.

For all of the treatments except for the control group, the densification process was pre-set in the computer control system. Steam was continuously injected during the whole process at a maximum manometer pressure of 550 kPa while the specimens were pressed under an increasing mechanical manometer platen pressure up to 6 MPa. The evolution of steam pressure and platen pressure during the whole process was previously presented in [20]. The whole densification process was divided into ten steps according to the treatment time (0, 5, 10, 15, 20, 25, 30, 35, 40 and 45 min). The density, gas permeability and thermal conductivity of samples densified at each treatment time and the control samples were determined, to fellow their variation during the THM densification process. For the samples densified for 5 min, the control system stopped at 5 min after the two hot platens closed, even though the maximum platen pressure had not been reached [20]. For the other treatments, the control system stopped at 10, 15, 20, 25, 30, 35, 40, 45 min, respectively, with both the maximum steam pressure and platen pressure being reached. All of the treated samples were then stored in a conditioning room at 20 °C and 65% RH until their equilibrium moisture content was reached prior to their properties determination.

2.2. Properties determination - Oven-dry average density

Three specimens for each densification time with dimensions 50 mm × 50 mm were oven dried and used to measure the density using an X-ray densitometer (Quintek Measurements Systems model QDP-01X, Knoxville, Tennessee, USA) at intervals of 0.02 mm through the thickness. The average value (n = 3) was used as the final oven-dry density of each group.

2.3. Permeability measurement

Three discs of 50 mm in diameter at each densification time level were prepared for the gas permeability measurement. A special device developed in our laboratory by Lihra et al. [7] was used to measure the transverse gas permeability of the wood samples. The gas permeability was measured in this study with air using the apparatus shown in Figure 2. A cylinder of compressed air equipped with a pressure regulator was used to regulate the flow of gas at the desired pressure. In addition, a silicon seal was used on the edge of each disc in order to make a tight seal with a rubber sleeve surrounding it. A pressure of 600 kPa was applied to the rubber sleeve to prevent air leaks through

Preprints (www.preprints.org) | NOT PEER-REVIEWED | Posted: 10 July 2018 doi:10.20944/preprints201807.0184.v1

the specimen edge. Two basswood discs (*Tilia americana*) with high longitudinal gas permeability were placed both in the inlet and outlet sides of the specimen to distribute the air flow [8]. Five flowmeters (Figure 2) with increasing range were installed to measure the gas flow rate through the samples. For each measurement, the flowmeter with a larger range (flowmeter 5) was firstly used. If there was no value provided, it was closed and the next one was used. This procedure was repeated until the gas flow rate could be measured. Each disc (n = 3 for each group) was measured at four pressure levels (ΔP - values measured from pressure gage B): 200, 250, 300 and 350 kPa, respectively.

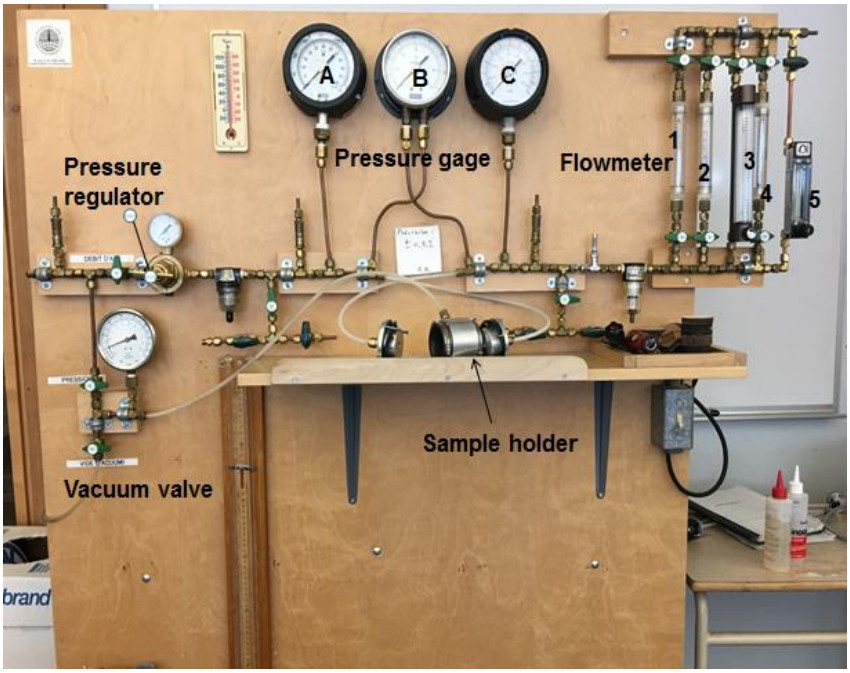

Figure 2. Apparatus used for gas permeability measurements.

The steady-state gas flow through wood can be characterized by Darcy's law. It could be stated as:

$$k_p^* = \frac{Q_g L}{A_s \Delta P} \frac{P}{\bar{P}} \quad (1)$$

Where k_p^* is apparent gas permeability with slip flow ($m_{gas}^3\ m_{wood}^{-1}\ s^{-1}\ Pa^{-1}$), Q_g is volumetric gas flow rate (m^3/s), L is the length in flow direction, corresponding to the thickness of sample (m), As is gas flow area (m^2), ΔP is the pressure differential between the inlet side and outlet side (Pa) (ΔP = P1 - P2), P1 is the inlet air pressure (Pa), P2 is the outlet air pressure (Pa), P is the pressure at which Q_g was measured (Pa), $\bar{P}$ is the arithmetic average pressure (Pa), $\bar{P} = \frac{(P_1+P_2)}{2}$.

The apparent gas permeability k_p^* from Eq.1 includes Knudsen diffusion, also named slip flow. When a gas flows through a capillary whose diameter is in the same order of magnitude as the average free path between the gas molecules, slip flow becomes significant and must be considered in the permeability measurement. The gas permeability corrected for slip flow could be obtained from the Klinkenberg equation [21]:

$$k_p^* = k_p * s \quad (2)$$

$$s = 1 + \frac{3.8\lambda}{r} \quad (3)$$

$$\lambda = \frac{2\mu}{\bar{P}} \sqrt{\frac{RT}{M_a}} \quad (4)$$

$$K = k_p * \mu \quad (5)$$

Preprints (www.preprints.org) | NOT PEER-REVIEWED | Posted: 10 July 2018 doi:10.20944/preprints201807.0184.v1

Where k_p is the apparent gas permeability corrected for slip flow (m_{gas}^3 m_{wood}^{-1} s^{-1} Pa^{-1}), s is the slip flow factor, λ is the average free path between gas molecules (m), r is the diameter of the capillary, R is the universal gas constant (8.31 J/mol/K), T is the absolute temperature (K), M_a is the molecular weight of air (kg/mol). K is the intrinsic gas permeability (m_{gas}^3 m_{wood}^{-1}), μ is viscosity of fluid (Pa·s) (for air at room temperature $\mu = 1.845 \times 10^{-5}$ Pa·s). k_p represents the "true" gas permeability corrected for slip flow and can be determined graphically from the intercept of a plot of k_p^* against the reciprocal average pressure ($1/\overline{P}$)[7,21].

2.4. Thermal conductivity measurement

Four specimens for each densification time with dimensions 152.4 mm × 170.0 mm were prepared for thermal conductivity measurement using the apparatus LaserComp Fox 314 (TA instruments, New Castle, USA) shown in Figure 3a. The Fox 314 instrument was designed according to the ASTM C 518-04 standard test method for steady-state thermal transmission properties by means of the heat flow meter apparatus. The specimen was placed between two heating plates (Figure 3b) with different temperature for a sufficient length of time to obtain a uniform temperature gradient throughout the sample. The temperature of the upper heating plate was set at 10 °C and that of the base heating plate was set at 35 °C. The temperature equilibrium of the system is considered to be reached when the temperatures of the two plates are stable within +/- 0.2 °C after the set point has been reached. During the test, the auto thickness mode was selected, and the sample's thickness was determined automatically by the instrument's precise digital thickness measurement system.

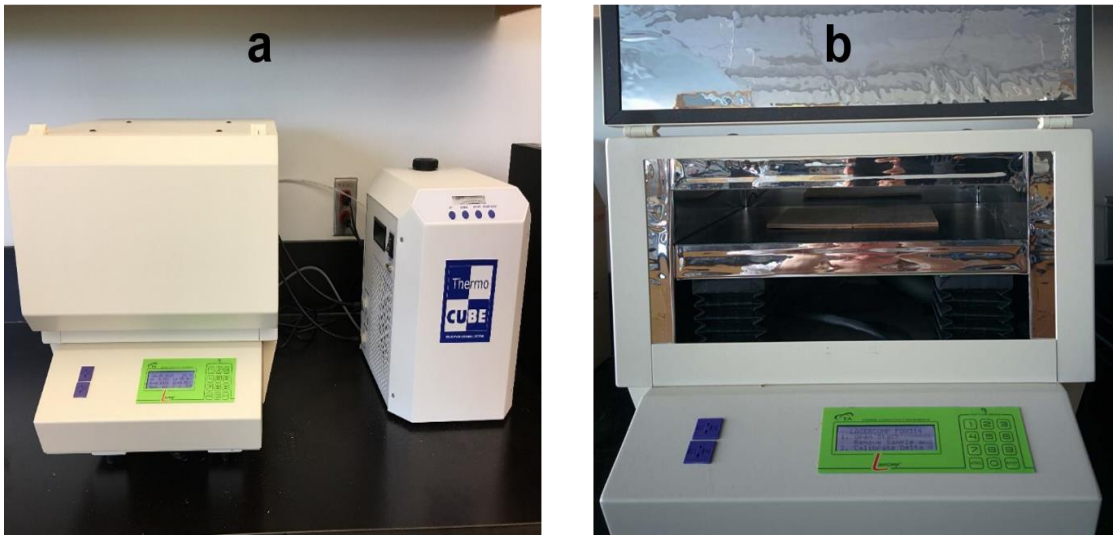

Figure 3. (a) Thermal conductivity testing apparatus; (b) Position of the sample and two heating plates.

The thermal conductivity is significantly affected by MC. To investigate the influence of MC on the thermal conductivity, each specimen (n = 4 for each group) was measured at three moisture content levels (0%, 6% and 12%), respectively. Finally, the thermal conductivity was described as a function of densification time and MC.

2.5. Statistical analysis

An analysis of variance (ANOVA) was performed to investigate the effect of densification time on the oven-dry density and gas permeability, and the effects of the densification time and MC on the thermal conductivity of densified sugar maple wood using SAS 9.4 (Cary, NC, USA) at significance level α=0.05. Duncan's test was conducted for multiple comparisons between average values obtained under different treatments.

3. Results

Preprints (www.preprints.org) | NOT PEER-REVIEWED | Posted: 10 July 2018 doi:10.20944/preprints201807.0184.v1

3.1. Oven-dry density

Figure 4 presents the evolution of the oven-dry density and thickness of the samples during the THM densification process. It can be seen that the thickness of the samples decreases in general with densification time. Most of the thickness reduction occurred within the first 5 - 15 min. This main reduction of thickness may be caused by the decrease of the void volume, and consequently resulted in an increase of the oven-dry density. However, the oven-dry density did not present a linear increase with the decrease of thickness.

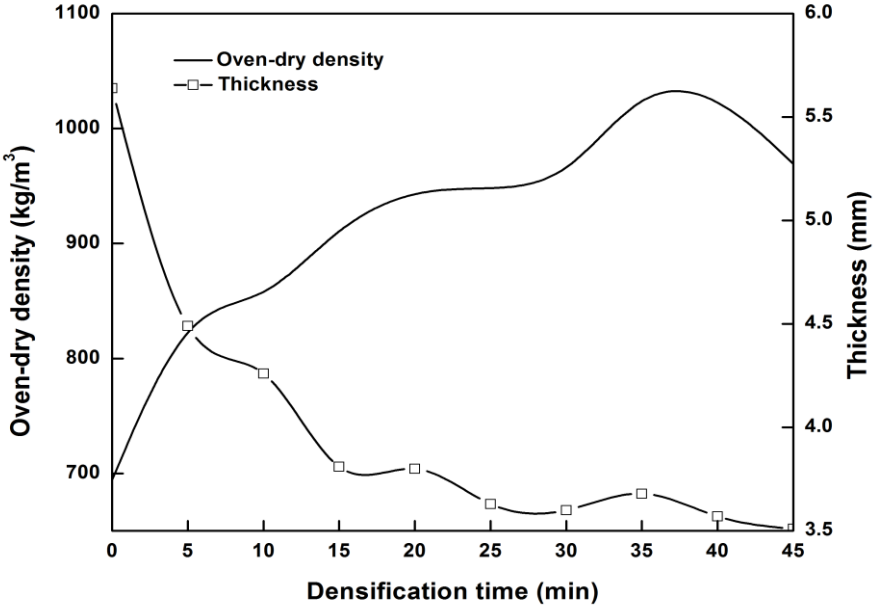

Figure 4. Variation of the average oven-dry density (n=3) and thickness (n=3) of wood during the densification process.

Typical density profiles of the control sample (densification time = 0 min) and samples densified for 10 min and 40 min, respectively, were selected to further investigate the density distribution of sample through its thickness undergoing different densification time treatments. As shown in Figure 5, the density of the control sample was almost constant throughout the thickness, with the exception of the lower density values observed on both surfaces. The samples densified for 10 min showed a higher density in the core than at the surface, this might have been caused by the large spring back after the press opening. In our previous research [22], the density profile of the samples densified at lower temperatures (180 °C and 190 °C) without steam showed similar tendency. This result also suggested that densification for 10 min was not enough, as the compressed deformation was not stable. The compressed sample surface experienced large spring back, resulting in a non-homogeneous density distribution. The density was more homogeneous in the core for the samples densified for 40 min, and a higher density at the surface than in the core was found. These observations were the same for samples densified at 200 °C with steam [22]. The heat distribution across the transverse direction was likely more homogeneous for samples densified for longer time with steam.

Preprints (www.preprints.org) | NOT PEER-REVIEWED | Posted: 10 July 2018 doi:10.20944/preprints201807.0184.v1

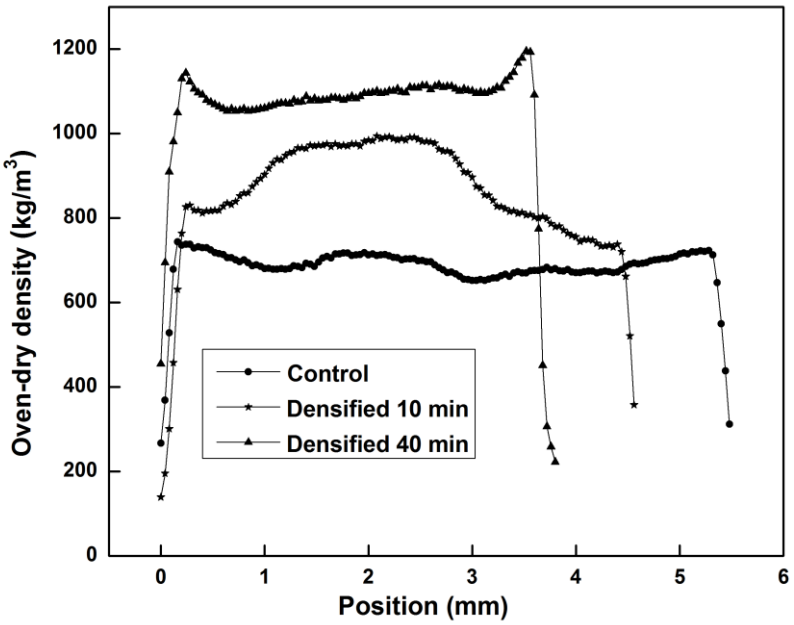

Figure 5. Typical density profile of wood samples densified at different time.

Analysis of variance results of average oven-dry density versus densification time are presented in Table 1. Which shown that the densification time had a significant effect on the oven-dry density ($p = 0.0002$). Table 2 presents the oven-dry density value of the control and densified samples, and the results of Duncan's test for all the treatments. It reveals that the main increase of the oven-dry density occurred during the first 5 - 15 min. When the densification time is over 40 min, the oven-dry density decreased, which might be caused by the degradation of hemicelluloses.

Table 1. Analysis of variance results of oven-dry density versus densification time.

Source	Sum of squares	DF	Mean square	F value	P value	Remarks
Densification time	280224.4	9	31136.0	6.8	0.0002	Significant

Table 2. Oven-dry density of the control and samples densified at different time.

Treatment time (min)	Oven-dry density (kg/m3) (n = 3)
0	694.3 (4.1)^{c*}
5	848.6 (82.8)^{b}
10	845.4 (76.1)^{b}
15	917.3 (61.0)^{ab}
20	948.3 (106.2)^{ab}
25	947.1 (43.5)^{ab}
30	952.7 (81.9)^{ab}
35	1039.6 (60.6)^{a}
40	1031.6 (44.2)^{a}

Preprints (www.preprints.org) | NOT PEER-REVIEWED | Posted: 10 July 2018 doi:10.20944/preprints201807.0184.v1

45	969.5 (65.6)^{ab}

Values in parenthesis are standard deviations; *: Duncan's test results, average values with the same letter indicate no significant difference at α = 0.05.

3.2. Permeability

A plot of k_p^* against $1/\overline{P}$ was made for each sample to correct the effect for slip flow. Figure 6 presents a typical relationship of the k_p^* against $1/\overline{P}$ for radial flow of the control sample. A slight linear relationship was observed in figure 6, indicating the occurrence of slip flow. Therefore, the measured values of k_p^* should be corrected for slip flow to obtain the gas permeability k_p from the intercept of the plot of k_p^* against $1/\overline{P}$ [7,21].

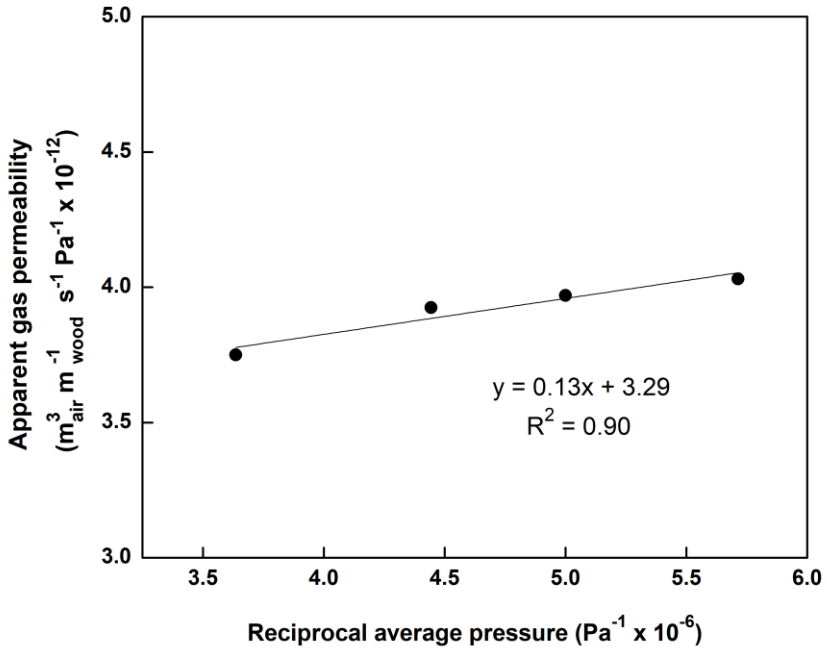

Figure 6. Typical relationship of the apparent gas permeability against the reciprocal average pressure for radial flow of the control sample.

The evolution of radial intrinsic gas permeability during the THM densification process is presented in Figure 7. Analysis of variance results of intrinsic gas permeability versus densification time are presented in Table 3. Table 4 presents the intrinsic gas permeability values of the control and densified samples, and the results of Duncan's test for all of the treatments.

The radial intrinsic gas permeability of the control sugar maple wood sample with an average oven-dry density of 694.3 kg/m^3 is 5.93 × 10^{-17} m^3_{air}/m_{wood}. As shown in Figure 7 and Table 4, the intrinsic gas permeability of wood decreased rapidly at the beginning of the densification treatment compared with that of the control sample. However, no statistical difference was found between the intrinsic gas permeability of samples densified at 5, 10 and 15 min, which might be due to their densities which were not significantly different. From 20 to 45 min, the intrinsic gas permeability decreased with increasing of densification time. The intrinsic gas permeability of the control sample could be 5 to 40 times greater than that of densified sample, which suggested that the void volume of wood reduced notably after densification.

Preprints (www.preprints.org) | NOT PEER-REVIEWED | Posted: 10 July 2018 doi:10.20944/preprints201807.0184.v1

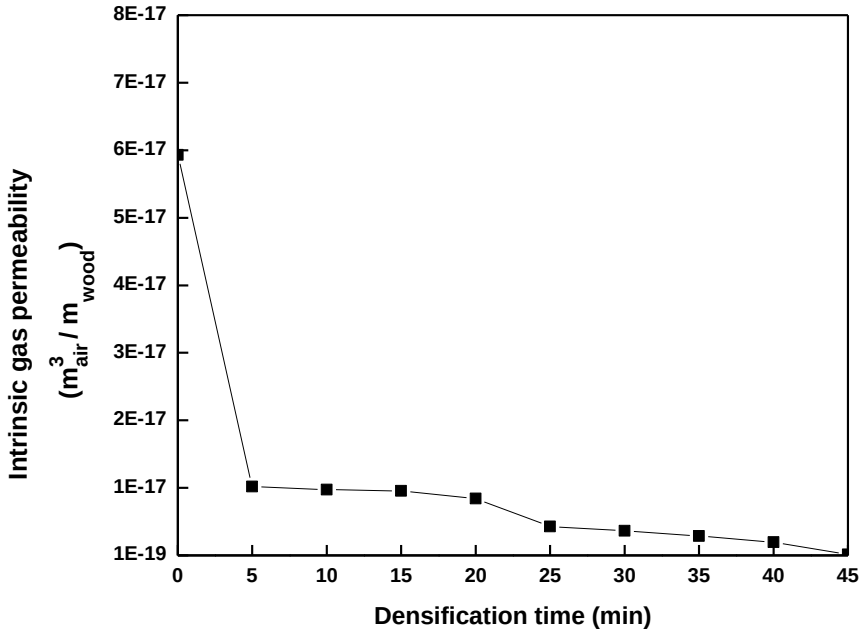

Figure 7. Evolution of the radial intrinsic gas permeability during the densification process.

It might be caused by the large difference between the radial intrinsic gas permeability of the control and densified samples, the whole data did not meet the assumption of a normal distribution. After performing normality test using SAS, it was found that a logarithm transformation (log_{10}) was needed. Table 3 revealed that the densification time had also a significant effect on wood permeability ($p < 0.0001$).

Table 3. Analysis of variance results of the radial intrinsic gas permeability versus densification time.

Source	Sum of squares	DF	Mean square	F value	P value	Remarks
Densification time (data after logarithmic transformation treatment)	5.9	9	0.66	22.61	<0.0001	Significant

Table 4. Radial intrinsic gas permeability of the control and samples densified for different times.

Treatment time (min)	Oven-dry density (kg/m³) (n = 3)	Intrinsic gas permeability (m^3_{air}/m_{wood}) (n = 3)	Intrinsic gas permeability (after logarithm transformation)
0	694.3 (4.1)^{c*}	5.93×10^{-17} (2.57×10^{-18})	-16.23^{a*}
5	848.6 (82.8)^{b}	1.02×10^{-17} (4.71×10^{-18})	-17.02^{b}
10	845.4 (76.1)^{b}	9.74×10^{-18} (2.48×10^{-18})	-17.02^{b}
15	917.3 (61.0)^{ab}	9.53×10^{-18} (4.95×10^{-18})	-17.06^{b}
20	948.3 (106.2)^{ab}	8.40×10^{-18} (4.19×10^{-18})	-17.12^{bc}
25	947.1 (43.5)^{ab}	4.28×10^{-18} (1.76×10^{-18})	-17.40^{cd}

Preprints (www.preprints.org) | NOT PEER-REVIEWED | Posted: 10 July 2018 doi:10.20944/preprints201807.0184.v1

30	952.7 (81.9)^{ab}	3.63×10^{-18}(2.00×10^{-19})	-17.44^{de}
35	1039.6 (60.6)^{a}	2.87×10^{-18} (1.64×10^{-18})	-17.58^{def}
40	1031.6 (44.2)^{a}	1.95×10^{-18} (4.8×10^{-19})	-17.72^{ef}
45	969.5 (65.6)^{ab}	1.4×10^{-18} (0.84×10^{-19})	-17.86^{f}

Values in parenthesis are standard deviations; *: Duncan's test results, average values with the same letter indicate no significant difference at α = 0.05.

3.3. Thermal conductivity

Table 5 shows the analysis of variance results of thermal conductivity versus densification time and MC. The thermal conductivity values of the control samples and densified samples are presented in Table 6. Table 5 reveals that both densification time and MC had significant effect on the thermal conductivity, but the interaction between the densification time and MC was not significant.

Table 5. Analysis of variance results of thermal conductivity versus densification time and moisture content.

Source	Sum of squares	DF	Mean square	F value	P value	Remarks
Densification time	0.014	9	0.002	38.88	<0.0001	Significant
Moisture content	0.001	2	0.001	19.18	<0.0001	Significant
Densification time * Moisture content	0.0002	18	0	0.24	0.99	

There is a common agreement that the MC has an important effect on wood thermal conductivity. As shown in Table 6, for all of the treatment times, the thermal conductivity increased with increasing MC. It could be found that the thermal conductivity increased by 0.5 - 1.5% per percent increase of MC for densified sugar maple wood. In particular, it can be noticed that the thermal conductivity of densified samples is slightly lower than that of the control samples. This was not expected given that wood thermal conductivity generally increases with increasing density [1,12]. However, according to ThermoWood Handbook [23], the thermal conductivity of heat treated wood (230 °C, 3 - 5 h) is reduced by 20 - 25% compared with normal untreated softwoods (pine and spruce). The underlying reasons for the decrease in thermal conductivity after densification treatment are not entirely clear. It might be due to the alteration of the crystalline structure of cellulose chains at higher treatment temperature, resulting in strength loss and changes in its ability to conduct heat at the cellular level [16].

Table 6. Thermal conductivity of the control and samples densified at different time.

Treatment time (min)	Oven-dry density (kg/m^3) (n = 3)	Thermal conductivity (W·m^{-1}·K^{-1}) (MC = 0%) (n = 4)	Thermal conductivity (W·m^{-1}·K^{-1}) (MC = 6%) (n = 4)	Thermal conductivity (W·m^{-1}·K^{-1}) (MC = 12%) (n = 4)
0	694.3 (4.1)^{c*}	0.124(0.008)^{b*}	0.130(0.005)^{b}	0.140(0.002)^{a}
5	848.6 (82.8)^{b}	0.097(0.006)^{cdefgh}	0.102(0.005)^{cdef}	0.106(0.006)^{c}
10	845.4 (76.1)^{b}	0.095(0.009)^{defgh}	0.098(0.010)^{cdefgh}	0.103(0.009)^{cde}
15	917.3 (61.0)^{ab}	0.096(0.009)^{cdefgh}	0.099(0.009)^{cdefg}	0.105(0.008)^{cd}
20	948.3 (106.2)^{ab}	0.094(0.005)^{efgh}	0.096(0.005)^{cdefgh}	0.101(0.005)^{cdefg}

25	947.1 (43.5)^{ab}	0.092(0.008)^{efgh}	0.094(0.007)^{defgh}	0.099(0.008)^{cdefg}
30	952.7 (81.9)^{ab}	0.091(0.004)^{fgh}	0.094(0.002)^{defgh}	0.099(0.002)^{cdefg}
35	1039.6 (60.6)^{a}	0.090(0.002)^{gh}	0.093(0.002)^{efgh}	0.099(0.004)^{cdefg}
40	1031.6 (44.2)^{a}	0.095(0.005)^{defgh}	0.097(0.005)^{cdefgh}	0.100(0.006)^{cdefg}
45	969.5 (65.6)^{ab}	0.088(0.007)^{h}	0.093(0.004)^{efgh}	0.096(0.005)^{cdefgh}

Values in parenthesis are standard deviations; *: Duncan's test results, average values with the same letter indicate no significant difference at α = 0.05

4. Discussion and Conclusions

THM is a feasible process to increase significantly the density of maple wood in a relative short time. Most of the oven-dry density increase occurred within the first 5 - 15 min of treatment. However, the oven-dry density did not show a linear increase with the decrease of thickness. The samples densified for 10 min showed a higher density in the core than at the surface, this might have been caused by the large spring back after the press opening. The heat distribution across the transverse direction was more homogeneous for samples densified for longer time with steam. The intrinsic gas permeability of the control samples was 5 to 40 times higher than that of densified wood. This indicated that the voids of wood reduced notably after the densification treatment. The thermal conductivity increased by 0.5 - 1.5% per percent increase of moisture content for densified sugar maple wood. The thermal conductivity of densified samples was lower than that of the control samples. The densification time had significant effects on oven-dry density and gas permeability. Both densification time and moisture content had significant effects on thermal conductivity, but their interaction effect was not significant.

Author Contributions: Qilan Fu carried out the experimental tests and prepared the manuscript. Alain Cloutier and Aziz Laghdir contributed to the experimental design and revised the manuscript. All authors read, discussed and approved the final manuscript.

Funding: This research was funded by the Natural Sciences and Research Council of Canada (NSERC) for funding this research under Discovery Grant No. 121954-2012.

Acknowledgments: The authors thank Mr. David Lagueux for technical assistance with the densification process.

Conflicts of Interest: The authors declare no conflict of interest.

References

1. Siau, J.F. *Transport Processes in Wood*, Timell, T.E. Eds.; Springer-Verlag, Heidelberg, Germany, 1984; ISBN-13:978-3-642-69215-4.
2. Dai, C.P.; Yu, C.M.; Zhou, X.Y. Heat and mass transfer in wood composite panels during hot pressing. Part II. Modeling void formation and mat permeability. *Wood Fiber Sci.* **2005**, *37*, 242-257.
3. Comstock, G.L. Directional permeability of softwoods. *Wood Fiber Sci.* **2007**, *1*, 283-289.
4. Denisov, O.B.; Anisov, P.P.; Zuban, P.E. Untersuchung der permeabilität von spanvliesen. *Holztechnologie* **1975,** *16*, 10-14.
5. Hata, T.; Kawai, S.; Ebihara, T.; Sasaki, H. Production of particleboards with a steam-injection press. Part V. Effects of particle geometry on temperature behaviors in particle mats and on air permeabilities of boards. *Mokuzai Galdcaishi* **1993,** *39*, 161-168.
6. Von Haas, G. Investigations of the hot pressing of wood-composite-mats under special consideration of the compression-behavior, the permeability, the temperature-conductivity and the sorption-speed. Doctoral Dissertation, University of Hamburg, Hamburg, Germany, 1998.
7. Lihra, T.; Cloutier, A.; Zhang, S.Y. Longitudinal and transverse permeability of balsam fir wetwood and normal heartwood. *Wood Fiber Sci*. **2000**, *32*, 164-178.

8. García, R.A.; Cloutier, A. Characterization of heat and mass transfer in the mat during the hot pressing of MDF panels. *Wood Fiber Sci.* **2005**, *37*, 23-41.
9. Defo, M.; Cloutier, A.; Fortin, Y. Modeling vacuum-contact drying of wood: The water potential approach. *Dry Technol.* **2000**, *18*, 1737-1778, DOI: 10.1080/07373930008917809.
10. Thömen, H. Modeling the physical processes in natural fiber composites during batch and continuous pressing. PhD thesis, Oregon State University, Corvallis, Oregon, 2000.
11. Gu, H.M.; Zink-Sharp, A. Geometric model for softwood transverse thermal conductivity. Part I. *Wood Fiber Sci.* **2005**, *37*, 699-711.
12. Simpson, W.; TenWolde, A. Moisture relations and physical properties of wood. In *Wood Handbook: Wood as an Engineering Material*. Ross, R.J.; Eds.; USDA forest service, Forest products laboratory, Madison, Wisconsin, 2010; pp. 4-11, ISBN-1523113464, 9781523113460.
13. Troppová, E.; Švehlík, M.; Tippner, J.; Wimmer, R. Influence of temperature and moisture content on the thermal conductivity of wood-based fibreboards. *Mater Struct.* **2015**, *48*, 4077-4083, DOI: 10.1617/s11527-014-0467-4.
14. Griffiths, E.; Kaye, G.W.C. The measurement of thermal conductivity. *P R Soc Lond A-Conta.* **1923**, *104*, 71-98, DOI: 10.1098/rspa.1923.0095.
15. MacLean, J. Thermal conductivity of wood. *Heat-Piping-Air Cond.* **1941**, *13*, 380-391.
16. Suleiman, B.M.; Larfeldt, J.; Leckner, B.; Gustavsson, M. Thermal conductivity and diffusivity of wood. *Wood Sci Technol.* **1999**, *33*, 465-473.
17. Haselein, C.R. Numerical simulation of pressing wood-fiber composites. PhD thesis, Oregon State University, Corvallis, Oregon, 1998
18. Fang, C.H.; Blanchet, P.; Cloutier, A.; Barbuta, C. Engineered wood flooring with a densified surface layer for heavy duty use. *BioResources* **2012a**, *7*, 5843-5854, DOI: 10.15376/biores.7.4.5843-5854.
19. Fang, C.H.; Mariotti, N.; Cloutier, A.; Koubaa. A.; Blanchet, P. Densification of wood veneers by compression combined with heat and steam. Eur J Wood Wood Prod. 2012b, 70, 155-163, DOI: 10.1007/s00107-011-0524-4.
20. Fu, Q.; Cloutier, A.; Laghdir, A. Optimization of the thermo-hygromechanical (THM) process for sugar maple wood densification. *BioResources* **2016**, *11*, 8844-8859, DOI: 10.15376/biores.11.4.8844-8859.
21. Siau, J. F. Wood: Influence of moisture on physical properties. Dept. of Wood Science and Forest Products, Virginia Polytechnic Institute and State University, 1995; ISBN-[13] 9780962218101-[10] 0962218103.
22. Fu, Q.; Cloutier A.; Laghdir A. Effect of heat and steam on the mechanical properties and dimensional stability of thermo-hygromechanically densified sugar maple wood. *BioResources* **2017**, *12*, 9212-9226, DOI: 10.15376/biores.12.4.9212-9226.
23. Finnish ThermoWood Association. ThermoWood Handbook. Helsinki, Finland, 2003.